

Development of Printable Natural Cartilage Matrix Bioink for 3D Printing of Irregular Tissue Shape

Chi Sung Jung¹ · Byeong Kook Kim¹ · Junhee Lee² · Byoung-Hyun Min^{1,3} · Sang-Hyug Park⁴ 

Received: 26 October 2017 / Revised: 10 November 2017 / Accepted: 22 November 2017 / Published online: 28 December 2017
© The Korean Tissue Engineering and Regenerative Medicine Society and Springer Science+Business Media B.V., part of Springer Nature 2017

Abstract The extracellular matrix (ECM) is known to provide instructive cues for cell attachment, proliferation, differentiation, and ultimately tissue regeneration. The use of decellularized ECM scaffolds for regenerative-medicine approaches is rapidly expanding. In this study, cartilage acellular matrix (CAM)-based bioink was developed to fabricate functional biomolecule-containing scaffolds. The CAM provides an adequate cartilage tissue-favorable environment for chondrogenic differentiation of cells. Conventional manufacturing techniques such as salt leaching, solvent casting, gas forming, and freeze drying when applied to CAM-based scaffolds cannot precisely control the scaffold geometry for mimicking tissue shape. As an alternative to the scaffold fabrication methods, 3D printing was recently introduced in the field of tissue engineering. 3D printing may better control the internal microstructure and external appearance because of the computer-assisted construction process. Hence, applications of the 3D printing technology to tissue engineering are rapidly proliferating. Therefore, printable ECM-based bioink should be developed for 3D structure stratification. The aim of this study was to develop printable natural CAM bioink for 3D printing of a tissue of irregular shape. Silk fibroin was chosen to support the printing of the CAM powder because it can be physically cross-linked and its viscosity can be easily controlled. The newly developed CAM-silk bioink was evaluated regarding printability, cell viability, and tissue differentiation. Moreover, we successfully demonstrated 3D printing of a cartilage-shaped scaffold using only this CAM-silk bioink. Future studies should assess the efficacy of *in vivo* implantation of 3D-printed cartilage-shaped scaffolds.

Keywords Extracellular matrix bioink · Cartilage matrix · Silk fibroin · 3D printing · Trochlea

✉ Byoung-Hyun Min
dr.bhmin@gmail.com

✉ Sang-Hyug Park
shpark1@pknu.ac.kr

¹ Departments of Molecular Science and Technology, Ajou University, 206, World Cup-ro, Yeongtonggu, Suwon 16499, Korea

² Department of Nature-Inspired Nano Convergence System, Korea Institute of Machinery and Materials, 156, Gajeongbuk-ro, Yuseong-gu, Daejeon 34103, Korea

³ Department of Orthopedic Surgery, School of Medicine, Ajou University, 206, World Cup-ro, Yeongtonggu, Suwon 16499, Korea

⁴ Department of Biomedical Engineering, Pukyong National University, 45, Yongso-ro, Namgu, Busan 48513, Korea

1 Introduction

The use of decellularized extracellular matrix (ECM) scaffolds for regenerative medicine approaches is rapidly expanding [1]. The ECM, which is secreted by the resident cells, consists of specific functional molecules and not only provides essential supportive structure but also generates significant biological cues that are required for tissue repair [2, 3]. In particular, the ECM binds growth factors and interacts with cell surface receptors to direct signal transduction and regulate gene transcription, thus managing essential morphological and physiological functions [4].

Numerous tissues and organs have now been decellularized for practical application of the ECM, and the latter has already been successfully used clinically for

regeneration of various tissues [5]. The ECM of each tissue provides a unique tissue-specific microenvironment for resident cells. The processes of cell attachment, migration, and proliferation are strongly influenced by the organization and structure of the unique ECM of each tissue. Because of these physical and biochemical properties, an ECM reproduces biochemical and mechanical properties of each organ such as tensile and compressive strength and elasticity.

In particular, the cartilage ECM is a structurally complex three-dimensional (3D) environment composed of various types of collagens and proteoglycans carrying various bioactive factors such as growth factors, integrins, and functional peptides [6]. Even very sophisticated and newly developed materials will never reach this complexity. In one study, a cartilage acellular matrix (CAM) was shown to provide a 3D environment suitable for attachment, proliferation, and chondrogenic differentiation of bone marrow-derived mesenchymal stem cells (BM-MSCs) [7]. Good scaffolds should offer a tissue-favorable environment and provide various shapes for new tissue regrowth. Nonetheless, conventional scaffold fabrication techniques do not meet these requirements for tissue regeneration [8, 9]. As an alternative to conventional scaffold manufacturing methods, 3D printing recently burst onto the scene of tissue engineering [10, 11]. 3D printing, based on computer-aided transfer processes, allows for better control of a scaffold's internal microstructure and external macro shape by means of several cell types, biomolecules, and biomaterials in contrast to conventional fabrication techniques [12–14]. Hence, applications of the 3D printing technology to tissue engineering are rapidly proliferating.

ECM materials are believed to have some of the most challenging characteristics in terms of 3D printing for tissue engineering [15]. To 3D-print biomaterials, the physical and mechanical properties should be reproduced in the printing process [16]. On the other hand, an ECM is difficult to print, and a printed ECM often has inadequate mechanical properties [17]. In an existing method that can overcome this limitation, polycaprolactone (PCL) is co-printed with an ECM material as a framework to enhance structural stability of the printed scaffold [15]. PCL can provide the desired mechanical properties and is easily tunable for tissue constructs. Nevertheless, several disadvantages of such synthetic polymers have also been recognized, for example, they have lower biodegradability and cell affinity than do natural polymers. Hence, a method for 3D printing is needed that is free of a synthetic framework for the ECM, which is essential for tissue regeneration. For 3D printing of an ECM without a framework, a natural polymer is suitable as a composite, given that natural

biomaterials are functionally superior to synthetic polymers because they are biocompatible and biodegradable.

Among natural-origin fibrous proteins, Silks from silkworms are abundant in nature [18] and it has been used for diverse applications with various forms [19, 20]. Silk proteins have found substantial applications in biomedicine owing to their high biocompatibility, tunable biodegradability, and good mechanical features [21]. In the present study, we developed a printable natural CAM-and-silk-based composite bioink for 3D printing of tissues with a specific shape. The proposed CAM-silk bioink was evaluated regarding printability, cell viability, and tissue differentiation by 3D printing a cartilage shape-mimicking scaffold for application to tissue engineering.

2 Materials and methods

2.1 Preparation of CAM materials

CAM materials were prepared from decellularized porcine articular cartilage. Briefly, the adherent soft tissues of articular cartilage were dissected and washed with phosphate-buffered saline (PBS). To decellularize the tissue, the cartilage pieces were pulverized using a freezer mill (JFC-300, JAI, Japan) and then treated with hypotonic buffer (10 mM Tris-HCl pH 8.0) for 12 h and with 1% sodium dodecyl sulfate (SDS) in TBS (Tris-buffered saline, 10 mM NaCl, pH 7.6) for 2 h. CAM was washed in deionized water by means of a centrifuge at 10,000 rpm for 20 min (five times) and then treated with DNase (100 U/ml, Elpis Biotech, Daejeon, Korea) for 12 h at 37°C. Next, another centrifugation step was applied (10,000 rpm for 20 min).

2.2 Preparation of silk fibroin

A silk fibroin solution was prepared from cocoons of the silkworm *Bombyx mori* (Tajima Shoji Co., Ltd., Yokohama, Japan) [22]. In brief, the cocoons were boiled in an aqueous solution of 0.02 M Na₂CO₃ for 30 min and rinsed thoroughly with distilled water to extract the adhesive sericin protein. The extracted fibroin was dissolved in a 9.3 M LiBr solution at 60°C for 4 h to obtain a 20 wt% aqueous solution. This solution was dialyzed against distilled water in Slide-a-Lyzer dialysis cassettes (molecular weight cutoff 3500; Pierce) at room temperature for 3 d to remove the salt.

2.3 Preparation of CAM-silk bioink and viscosity measurement

The resulting CAM powder at 5, 10, 15, 18, and 20% (w/v) was blended with an 8% (w/v) silk fibroin solution to prepare CAM-silk bioink.

The viscosity of the CAM-silk bioink was analyzed on a Brookfield DV-III Ultra Viscometer with a programmable rheometer and a programmable controller (TC-502P, Brookfield Engineering Laboratories, Middleboro, MA). The viscosity values of the 5, 10, 15, 18, and 20% CAM-silk bioink were compared with an 8% silk fibroin solution using a T-F spindle rotating at 0.2 rpm and 25°C.

2.4 Fabrication of 3D-printed scaffolds

We utilized the 3D-printing system established by the Nature-Inspired Nano Convergence System Department of the Korea Institute of Machinery and Materials (Daejeon, Korea). The extrusion optimized 18% CAM-silk bioink was utilized for 3D printing. Magnetic resonance imaging (MRI) data were converted to conventional stereolithography data in conversion software (mimics innovation suite, Materialise Medical, USA). The data were then converted to numerical control code containing driving information such as space, direction, height, and speed for nozzle floatation of the dispenser. In particular, a 3D-printing system based on air pressure and screw mixing of hydrogel polymers was used here for the CAM scaffold fabrication. The 3D-printing system consisted of x-, y-, and z-stages; air pressure; a screw mixing system; compression controller; and 3D data processing software. CAM-silk scaffolds were cross-linked with methanol only or 100 mM 1-ethyl-3-(3-dimethylaminopropyl) carbodiimide (EDC)/N-hydroxysuccinimide (NHS) in water (EDC-W) or in 80% methanol (EDC-M) for 12 h. After that, the unreacted functional groups were washed away with 5 mM sodium phosphate. All the experimental reagents were purchased from Sigma Chemical Co. (St. Louis, Mo, USA). The 3D-printing system contains extrusion head nozzles for printing. It was provided by the department responsible for the Nature-Inspired Nano Convergence System of Korea Institute of Machinery and Materials (Daejeon, Korea).

2.5 Scanning electron microscopy (SEM) analysis

To examine the morphology of the scaffolds, the specimens were freeze-dried and coated with gold and palladium and then examined by SEM (Stereoscan 440, Cambridge, UK) operated at 10 kV.

2.6 Mechanical properties

The compressive modulus of 3D-printed structures involving CAM-silk bioink or PCL was measured by means of a Universal Testing Machine (H5KT, Tinius-Olsen, Horsham, PA, USA). The specimens with a square shape of certain size ($10 \times 10 \times 3$ mm) were prepared. They were compressed at a constant rate of 1 mm/min using a 50-N load cell until each specimen broke.

2.7 Cell seeding

Rabbit bone marrow-derived mesenchymal stem cells (rBM-MSCs) were isolated from the thighs of 2-week-old female New Zealand white rabbits (IACUC no. 2013-0045). They were kindly provided by the Ajou Cell Therapy Center (Suwon, Korea). The obtained cells were passed through a nylon mesh cell strainer (BD Biosciences, Bedford, MA, USA) and centrifuged at $1500 \times g$ for 5 min. The cell pellet was resuspended in the MEM medium supplemented with 10% of fetal bovine serum (Hyclone, Logan, UT) and 1% of an antibiotic-antimitotic solution (Gibco). Second-passage rBM-MSCs were seeded at $8000/\text{mm}^3$ into ethanol-sterilized CAM scaffolds. Next, the construct was incubated for 3 weeks in a chondrogenic medium consisting of DMEM supplemented with 100 nM dexamethasone, 50 $\mu\text{g}/\text{ml}$ ascorbate-2 phosphate, ITS supplement, 40 $\mu\text{g}/\text{ml}$ proline, 25 mg/ml bovine serum albumin, and 100 $\mu\text{g}/\text{ml}$ sodium pyruvate. All reagents were purchased from Gibco fisher scientific. The culture medium was changed every 3 d during cultivation.

2.8 Cell compatibility

The cell seeding efficiency was confirmed by counting of unattached cells on the scaffolds after 3 h. The viability of cells attached to a scaffold was evaluated by a Live/Dead Cell Assay (Lonza, Walkersville, MD, USA) after 24 h. Briefly, each prepared specimen was incubated with 2 mM calcein AM (staining of live cells) and 4 mM EthD-1 (staining of dead cells) in PBS for 30 min at 5% (v/v) CO_2 at 37°C and was then washed with PBS. The stained cells were visualized and counted manually using a fluorescence microscope to determine the ratio of live cells to dead cells (Axiovert 200, Zeiss, Jena, Germany). The number of proliferating cells was also determined on Days 1, 3, 5, and 7 using a WST Assay (EZ-cytox; Daeil Lab Service, Seoul, Korea).

2.9 Histological analysis

The specimens were fixed at 4 °C in 4% phosphate-buffered paraformaldehyde, dehydrated in a graded series of

ethanol solutions and then embedded in paraffin wax for histological examination. Sectioned specimens (thickness 4 μm) were prepared and stained with safranin-O for glycosaminoglycan (GAG) analysis to confirm the chondrogenesis.

2.10 Statistical analysis

Data were expressed as mean \pm standard deviation (SD) from at least three independent experiments. Statistical significance was determined by one-way analysis of variance (ANOVA) followed by the Tukey–Kramer post hoc test. A difference with $p < 0.05$ was considered statistically significant.

3 Results

3.1 Printability test

Figure 1 showed printability test results that silk-only and 5, 10, and 15% CAM-silk bioinks could not be stacked line by line because of low viscosity. In contrast, 18% and 20% CAM-silk bioinks yielded fine-resolution filaments. Nonetheless, 20% CAM-silk bioink was so dense that it could not be smoothly extruded as a line (Fig. 1F, arrow). The viscosity of CAM-silk bioink was tested to analyze the physical properties. Although silk only and 5 and 10% CAM-silk bioinks were too watery to measure viscosity, the viscosity of 15, 18, and 20% CAM-silk bioinks was found to be 240, 2500, and 3700 Pa.s, respectively (Fig. 1G).

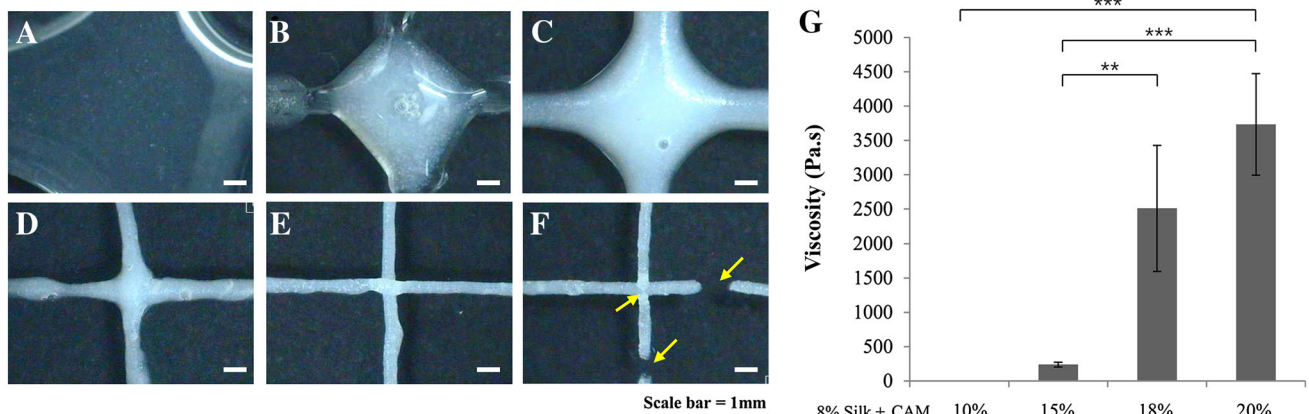


Fig. 1 Bioink printability testing. **A–F** Extrusion testing and **G** measurement of viscosity of CAM-silk bioinks. **A** 8% silk fibroin-only and **B** 5% CAM-silk, **C** 10% CAM-silk, **D** 15% CAM-silk, **E** 18% CAM-silk and **F** 20% CAM-silk bioinks. The silk-only and 5, 10, and 15% CAM-silk bioinks could not be stacked layer by layer. In

3.2 Mechanical strength analysis

Rectangular scaffolds (10 \times 10 \times 3 mm) made of CAM-silk or PCL (Fig. 2A) were printed for mechanical strength analysis. The pore size of the CAM-silk scaffold was 610 μm (Fig. 2A, top, and B). PCL scaffold had \sim 770- μm pore size (Table 1). Printed grid shapes were well maintained in both groups. The CAM-silk scaffold showed significantly lower compressive modulus (2.5 kPa) than the PCL scaffold did (30 kPa). Nonetheless, the CAM-silk scaffold had tunable mechanical properties via different cross-linking methods. In particular, EDC-M-treated scaffolds showed much greater mechanical strength than did methanol- or EDC-W-crosslinked scaffolds (Fig. 2B).

3.3 Degradation profiles of 3D-printed scaffolds

There were changes (Fig. 3) in shapes and weights of printed CAM-silk and PCL scaffolds in collagenase after incubation for 7 d. The non-cross-linked CAM-silk scaffolds collapsed after only 1 d in 0.2% collagenase. The extruded structures swelled and then were completely dissolved at the end of the incubation. Methanol and EDC-W groups showed similar degradation properties after 3–5 d. On the other hand, EDC-M and PCL groups appeared to well maintain the printed 3D structure (Fig. 3A). Quantitative analysis of dry weight confirmed that EDC-M scaffolds did not degrade after a week. EDC-W scaffolds retained \sim 20% of the initial weight (Fig. 3B).

3.4 The cell compatibility test

Cell-seeding efficiency was calculated by counting unattached cells 3 h after seeding. CAM-silk scaffolds showed

contrast, 18 and 20% CAM-silk bioinks could be extruded as a fine-resolution filament. Yellow arrows indicate the disconnected extruding lines of bioink. **G** Viscosity increased gradually with the amount of CAM added into the silk solution (** $p < 0.01$, *** $p < 0.001$)

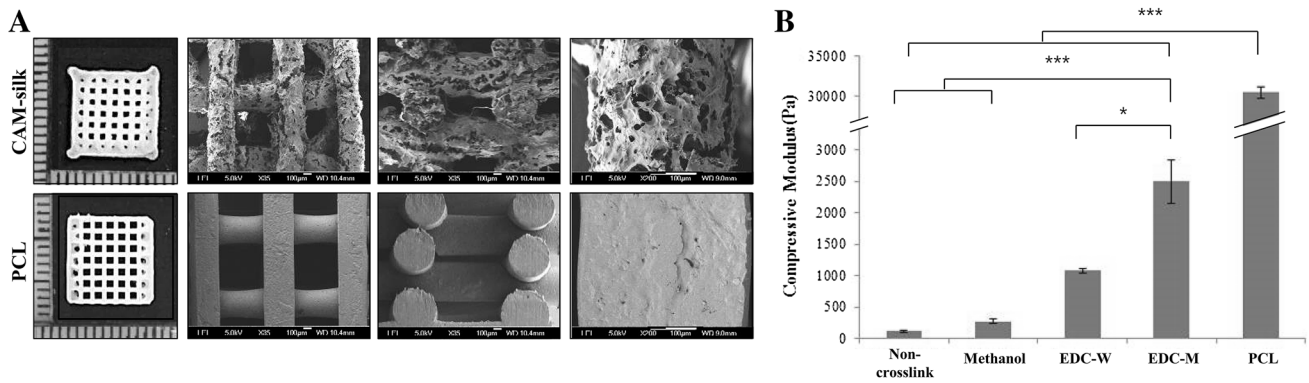


Fig. 2 Gross examination and mechanical-strength analysis. **A** Morphological features of printed rectangular scaffolds (10 × 10 × 3 mm). Thickness, grid interval, and porosity of the printed scaffolds were quantitatively analyzed in Table 1. **B** Mechanical-strength

analysis of the printed CAM-silk scaffolds. Compressive modulus of the CAM-silk scaffolds was tunable by varying the cross-linking method (**p* < 0.05, ****p* < 0.001)

Table 1 Structural characterizations of printed rectangular scaffolds

Structural property	CAM-silk	PCL
Grid interval (mm)	0.61 (±0.036)	0.77 (±0.016)
Thickness (mm)	0.57 (±0.046)	0.53 (±0.015)
Porosity (%)	89.5 (±0.4)	79.82 (±3.47)

statistically higher cell-seeding efficiency than PCL scaffolds did (Fig. 4A). Moreover, the growth rates of CAM-silk scaffolds were better than those of PCL scaffolds (Fig. 4B). To measure the cell viability, cell-seeded scaffolds were stained on Day 1 (Fig. 4C). Although the adhered-cell survival rate on the CAM-silk scaffolds was

over 80%, the other group (PCL scaffolds) showed cell viability of only ~ 60% (Fig. 4D).

3.5 Chondrogenesis of rBM-MSCs

Safranin-O staining was performed to confirm that the CAM-silk printed scaffold could induce the chondrogenesis of rBM-MSCs (red staining). Notably, seeded cells occupied the interior space of the CAM-silk scaffold after 1 week (arrows in Fig. 5). The CAM-silk printed scaffold showed intensive staining for cartilaginous synthesized GAGs under the same culture conditions after 3 weeks as compared to printed PCL scaffolds. Then, cell substrate synthesis was confirmed after 2 and 3 weeks, respectively (Fig. 5).

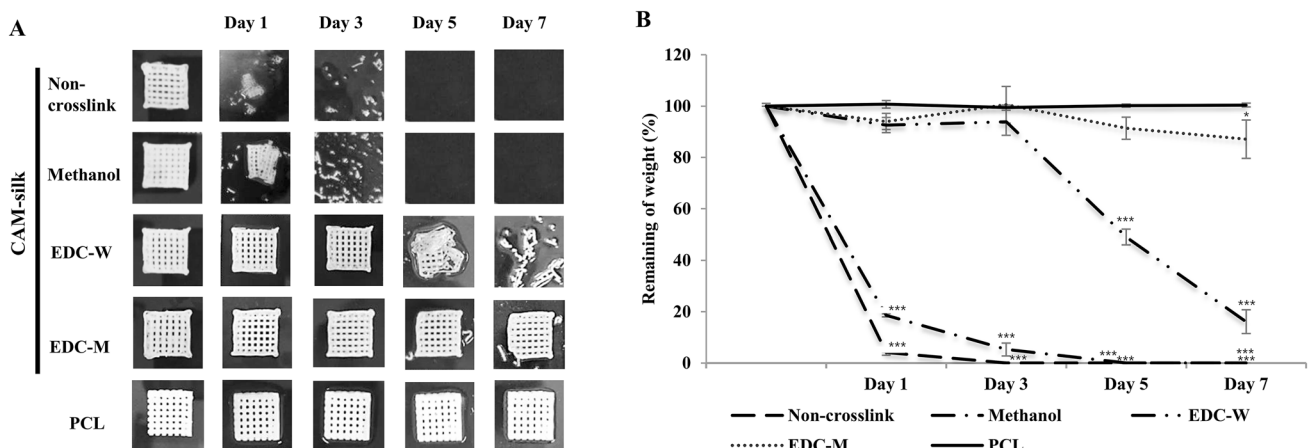


Fig. 3 Degradation profiles of 3D-printed scaffolds. **A** Gross shapes of CAM-silk and PCL scaffolds incubated for 7 d with collagenase. Although non-cross-linked CAM-silk scaffolds collapsed after only 1 d, EDC-M and PCL groups appeared to well maintain the printed 3D

structure. **B** Quantitative analysis of degradation of the 3D-printed scaffolds. EDC-M scaffolds did not degrade for over a week (**p* < 0.05, ****p* < 0.001)

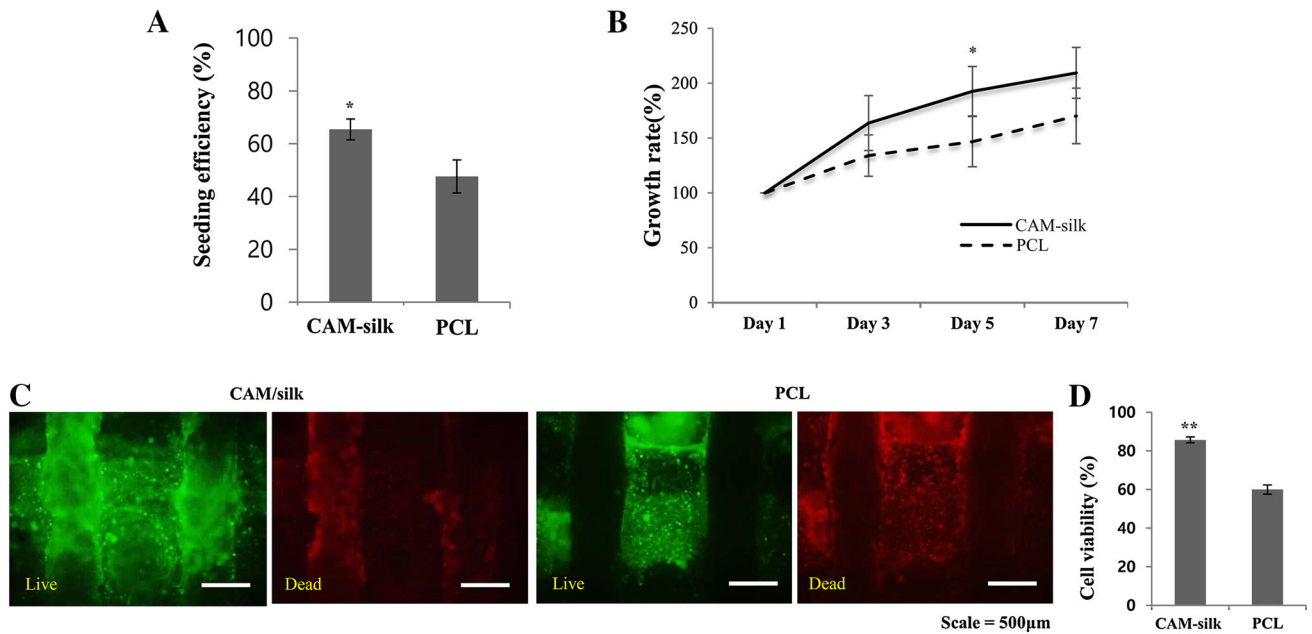


Fig. 4 Cell compatibility testing. **A** Cell-seeding efficiency of 3D-printed scaffolds. **B** Quantification of cell proliferation. Cell growth rates were evaluated by means of the WST-1 kit. **C** Cell viability analysis by staining. Live and dead cells were stained on the CAM-

silk and PCL scaffolds. **D** Quantitative analysis of cell viability. CAM-silk scaffolds yielded significantly higher cell viability than PCL scaffolds did (* $p < 0.05$, ** $p < 0.01$)

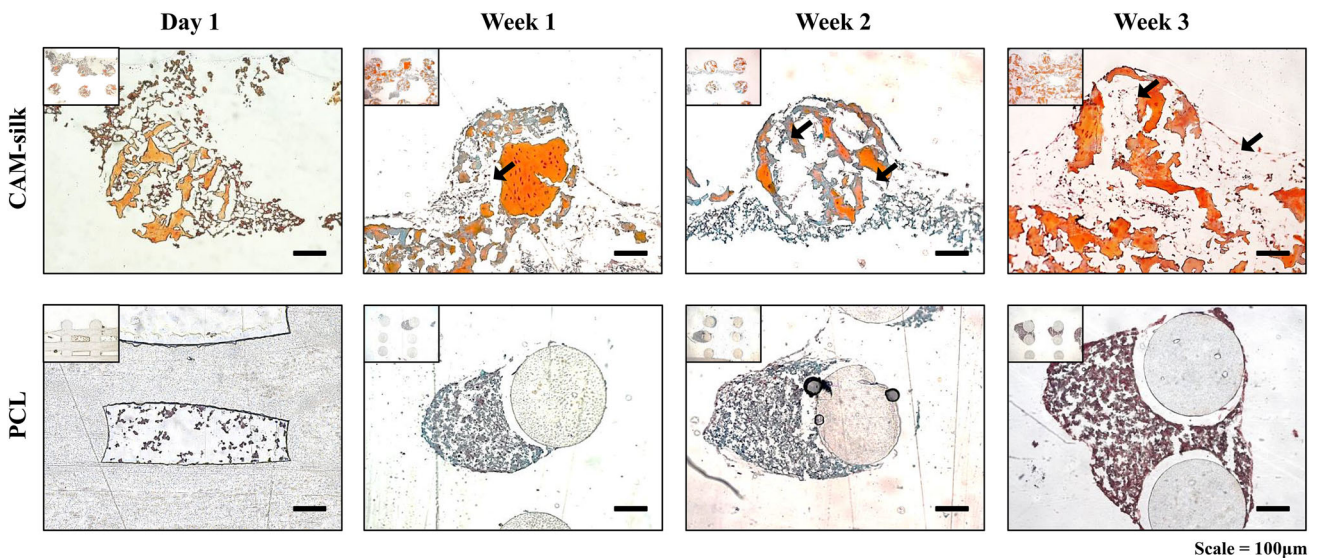


Fig. 5 Histological analysis of differentiation. Safranin-O staining was performed to confirm that the printed scaffolds could induce the chondrogenesis of rBM-MSCs. CAM-silk printed scaffold appeared

to intensively stain for cartilaginous synthesized GAGs under the same culture conditions on Day 21 as compared to printed PCL scaffolds

3.5.1 3D printing of the human articular cartilage shape

By means of the CAM-silk bioink, cartilage trochlea of irregular shape was printed successfully without supporting materials. The size of the printed trochlea scaffold was $4.5 \times 5 \times 3$ cm: 100% scale of the human articular cartilage (Fig. 6).

4 Discussion

In this study, we developed printable CAM-based bioink containing a silk fibroin solution to achieve 3D printing of a tissue of irregular shape. The CAM-silk bioink was confirmed to support a good cell response and chondrogenesis of rBM-MSCs. In addition, the irregular structure

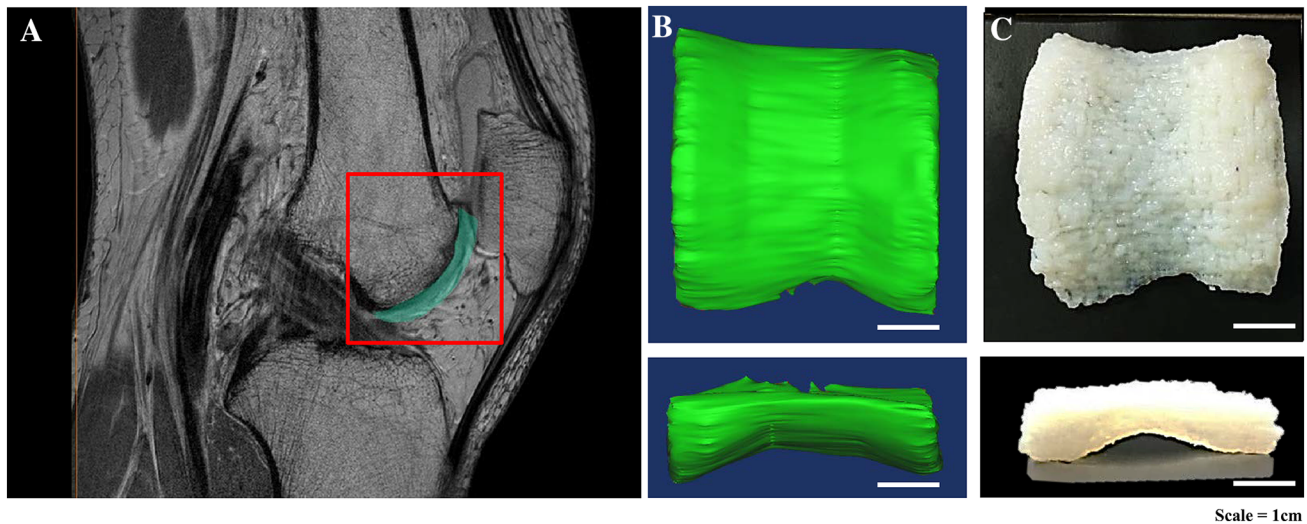


Fig. 6 Replication of the human articular trochlea cartilage. **A** Patient's MRI image, red square indicates the image reconstructing region of 3D modeling for trochlea shape printing. **B** 3D trochlea modeling on the basis of an MRI image with reproduction of the real

100% scale (curved cartilage). **C** 3D printed trochlea shape was imitated by the 3D-printing technique using CAM-silk bioink. By means of the CAM-silk bioink, the cartilage trochlea of irregular shape was printed successfully without supporting materials

of human cartilage was successfully mimicked using the newly developed bioink.

Biomaterials applicable to 3D printing must have not only adequate but also injectable viscosity to allow for structural lamination. Bioink with lower than the appropriate viscosity was injectable, but structural lamination was difficult. On the other hand, materials of higher viscosity could be stacked into a 3D structure, but linear printing was difficult. To optimize the printing conditions, a syringe test and viscosity measurement were conducted under various conditions (Fig. 1). We identified the optimal blending ratio—18% CAM powder with a 7% silk solution—for stable printability of CAM-silk bioink.

For 3D printing of a specific tissue shape, we needed to use high-resolution-compatible bioink that can modulate the internal structure and external shape. These properties can facilitate the nutrient supply and metabolic activity of the cells after formation of the tissue.

Printed scaffolds made of a constant extrusion material have well-interconnected pores [23]. Interconnected pore structures of our CAM-silk scaffolds showed no significant difference from those of PCL scaffolds, thus proving outstanding 3D printability. Besides, the proper material surface is an important condition for cell adhesion, survival, and tissue regeneration [24]. The printed PCL scaffold appeared to have a smooth surface without any pattern or porosity. Unlike PCL, the printed CAM-silk scaffold had a rough surface containing micropores (Fig. 2A). This surface of the material may support better cell adhesion and an improved response in terms of differentiation.

Stable mechanical properties are the most important factor for 3D printing to successfully mimic a tissue shape.

We showed that the newly developed CAM-silk scaffolds have much lower mechanical strength than PCL scaffolds do. Nevertheless, the mechanical strength of the CAM-silk material could be substantially improved by the modified cross-linking method. Regarding the degradability test, degradation of the PCL material was very slow and could not be adjusted even though PCL is a material known to be biodegradable [25]. On the other hand, the ECM scaffolds were confirmed to be amenable to adjustments of biodegradability. In particular, CAM-silk scaffolds cross-linked by the modified EDC-M method showed enzyme resistance similar to that of PCL scaffolds in the degradation test (Fig. 3). To confirm the cell response in the printed CAM-silk scaffolds, cell-seeding efficiency, viability, and proliferation were analyzed. The results confirmed that CAM-silk scaffolds provide better morphological changes and tissue formation from cells in comparison with printed PCL scaffolds during *in vitro* culture.

To date, natural materials have had limitations regarding printing of irregular tissue shapes without a supporting frame of synthetic materials like PCL because of unsuitable printability [26]. In the present study, we successfully created strongly curved cartilage-shaped scaffolds based on an actual patient's cartilage MRI data using only a printability-improved bioink consisting of a natural CAM powder blended with a silk solution. It can be predicted that the newly developed CAM-based bioink can be employed for morphological replication of other human tissues.

Finally, this study offers a natural bioink platform with an excellent tissue regeneration potential and capable of

tissue shape replication. Future studies should be focused on the development of a cell-based directly printable natural ECM bioink and on evaluation of *in vivo* efficacy of the implantation of 3D-printed tissue-shaped scaffolds.

Acknowledgements This research was supported by a grant of the Korea Health Technology R&D Project through the Korea Health Industry Development Institute (KHIDI), funded by the Ministry of Health and Welfare, Republic of Korea (HI14C2143 and HI14C0744).

Compliance with ethical standards

Conflicts of interest The authors have no financial conflicts of interest.

Ethical statement This research protocol was approved by the IACUC of Ajou University (IACUC no.2013-0045).

References

- Chan BP, Leong KW. Scaffolding in tissue engineering: general approaches and tissue-specific considerations. *Eur Spine J*. 2008;17:467–79.
- Bolland F, Korossis S, Wilshaw SP, Ingham E, Fisher J, Kearney JN, et al. Development and characterisation of a full-thickness acellular porcine bladder matrix for tissue engineering. *Biomaterials*. 2007;28:1061–70.
- Agmon G, Christman KL. Controlling stem cell behavior with decellularized extracellular matrix scaffolds. *Curr Opin Solid State Mater Sci*. 2016;20:193–201.
- Wade RJ, Burdick JA. Engineering ECM signals into biomaterials. *Mater Today (Kidlington)*. 2012;15:454–9.
- Scarritt ME, Pashos NC, Bunnell BA. A review of cellularization strategies for tissue engineering of whole organs. *Front Bioeng Biotechnol*. 2015;3:43.
- Benders KE, van Weeren PR, Badylak SF, Saris DB, Dhert WJ, Malda J. Extracellular matrix scaffolds for cartilage and bone regeneration. *Trends Biotechnol*. 2013;31:169–76.
- Yang Q, Peng J, Guo Q, Huang J, Zhang L, Yao J, et al. A cartilage ECM-derived 3-D porous acellular matrix scaffold for *in vivo* cartilage tissue engineering with PKH26-labeled chondrogenic bone marrow-derived mesenchymal stem cells. *Biomaterials*. 2008;29:2378–87.
- Park JH, Jang J, Lee JS, Cho DW. Three-dimensional printing in tissue engineering and regenerative medicine. *Tissue Eng Regen Med*. 2016;13:612–21.
- Ahn SH, Lee J, Park SA, Kim WD. Three-dimensional bioprinting equipment technologies for tissue engineering and regenerative medicine. *Tissue Eng Regen Med*. 2016;13:663–76.
- Park SH, Jung CS, Min BH. Advances in three-dimensional bioprinting for hard tissue engineering. *Tissue Eng Regen Med*. 2016;6:622–35.
- Peltola SM, Melchels FP, Grijpma DW, Kellomäki M. A review of rapid prototyping techniques for tissue engineering purposes. *Ann Med*. 2008;40:268–80.
- Shivalkar S, Singh S. Solid freeform techniques application in bone tissue engineering for scaffold fabrication. *Tissue Eng Regen Med*. 2017;14:187–200.
- Kim JH, Yoo JJ, Lee SJ. Three-dimensional cell-based bioprinting for soft tissue regeneration. *Tissue Eng Regen Med*. 2016;6:647–62.
- Sobral JM, Caridade SG, Sousa RA, Mano JF, Reis RL. Three-dimensional plotted scaffolds with controlled pore size gradients: effect of scaffold geometry on mechanical performance and cell seeding efficiency. *Acta Biomater*. 2011;7:1009–18.
- Pati F, Jang J, Ha DH, Won Kim S, Rhie JW, Shim JH, et al. Printing three-dimensional tissue analogues with decellularized extracellular matrix bioink. *Nat Commun*. 2014;5:3935.
- Murphy SV, Atala A. 3D bioprinting of tissues and organs. *Nat Biotechnol*. 2014;32:773–85.
- Combellack EJ, Jessop ZM, Naderi N, Griffin M, Dobbs T, Ibrahim A, et al. Adipose regeneration and implications for breast reconstruction: update and the future. *Gland Surg*. 2016;5:227–41.
- Jin HJ, Kaplan DL. Mechanism of silk processing in insects and spiders. *Nature*. 2003;424:1057–61.
- Liu W, Li Z, Zheng L, Zhang X, Liu P, Yang T, et al. Electrospun fibrous silk fibroin/poly(L-lactic acid) scaffold for cartilage tissue engineering. *Tissue Eng Regen Med*. 2016;13:516–26.
- Kundu B, Kurland NE, Bano S, Patra C, Engel FB, Yadavalli VK, et al. Silk proteins for biomedical applications: bioengineering perspectives. *Prog Polym Sci*. 2014;39:251–67.
- Floren M, Migliaresi C, Motta A. Processing techniques and applications of silk hydrogels in bioengineering. *J Funct Biomater*. 2016;7:E26.
- Park SH, Gil ES, Cho H, Mandal BB, Tien LW, Min BH, et al. Intervertebral disk tissue engineering using biphasic silk composite scaffolds. *Tissue Eng Part A*. 2012;18:447–58.
- Trachtenberg JE, Placone JK, Smith BT, Fisher JP, Mikos AG. Extrusion-based 3D printing of poly(propylene fumarate) scaffolds with hydroxyapatite gradients. *J Biomater Sci Polym Ed*. 2017;28:532–54.
- Tallawi M, Rosellini E, Barbani N, Cascone MG, Rai R, Saint-Pierre G, et al. Strategies for the chemical and biological functionalization of scaffolds for cardiac tissue engineering: a review. *J R Soc Interface*. 2015;12:20150254.
- Xia Y, Zhou P, Cheng X, Xie Y, Liang C, Li C, et al. Selective laser sintering fabrication of nano-hydroxyapatite/poly-epsilon-caprolactone scaffolds for bone tissue engineering applications. *Int J Nanomedicine*. 2013;8:4197–213.
- Guvendiren M, Molde J, Soares RM, Kohn J. Designing biomaterials for 3D Printing. *ACS Biomater Sci Eng*. 2016;2:1679–93.